This pdf file consists of figures containing photographs, and their captions, scanned from:

GEOLOGY AND $^{40}AR/^{39}AR$ GEOCHRONOLOGY OF THE COASTAL COMPLEX NEAR TROUT RIVER AND LARK HARBOUR, WESTERN NEWFOUNDLAND

by

Bruce D. Idleman

A Dissertation

Submitted to the State University of New York at Albany

in Partial Fulfillment of

the Requirements for the Degree of

Doctor of Philosophy

College of Science and Mathematics

Department of Geological Sciences

1990

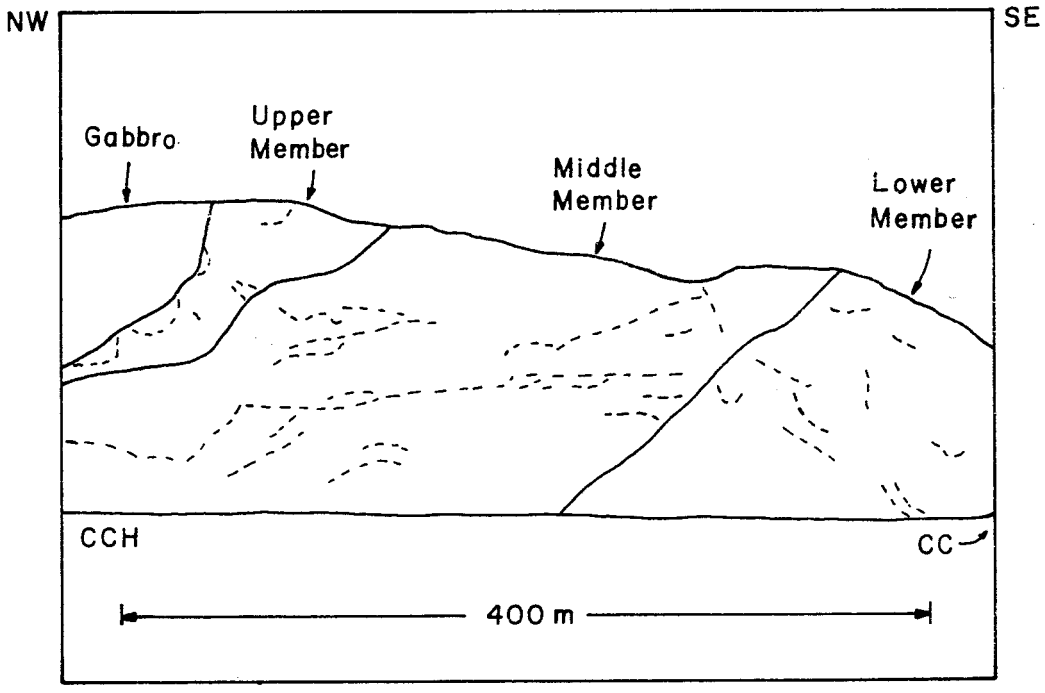

Figure 4.1

Photograph and corresponding sketch map showing the distribution of Skinner Cove lithologies between Chimney Cove (CC) and Chimney Cove Head (CCH).

Figure 4.2

Mafic pillow lava from the middle member of the Skinner Cove Formation near Chimney Cove. Sparry white calcite occurs both as veins and as interstitial fill between pillows in this exposure.

Figure 4.3

Massive mafic lava flows from the middle member of the Skinner Cove Formation north of Chimney Cove Head. The lowermost, dark grey flow contains abundant amygdules and veins of sparry white calcite. Strong hematization is evident in the uppermost, reddish-purple flow and portions of the greenish-grey flow beneath it.

Figure 4.4

Rounded cobbles of plagioclase-phyric mafic lava from the middle member of the Skinner Cove Formation near Chimney Cove. Pink to grey micritic limestone fills the interstices between some of the cobbles, particularly in the upper left corner of the photograph. Note the prominent spheroidal weathering and exfoliation in many of the cobbles.

Figure 4.5

Calcite-cemented mafic volcanic breccia from the middle member of the Skinner Cove Formation south of Chimney Cove Head.

Figure 4.6

Channel in mafic volcanics of the Skinner Cove Formation (middle member) south of Chimney Cove Head. The lowermost portion of the channel is filled with crudely bedded, pebbly, carbonate-cemented volcanic breccia that contains matrix-supported cobbles of mafic volcanic rock. The breccia grades upward into grey, carbonate-rich volcaniclastic sandstone and pinkish-grey sandy micrite.

Figure 4.7

Gabbro from the Skinner Cove Formation south of Bottle Cove. The gabbro (pale grey) contains a prominent igneous foliation that dips moderately toward the right (southeast). An undeformed diabase dike (darker grey) cuts the gabbro along the left side of the photograph.

Figure 4.8

Contact between gabbro (lower right) and mafic volcanic rock (upper left) of the Skinner Cove Formation south of Bottle Cove. The hammer head marks the position of the contact, which dips moderately toward the left (east). Note the oblique relationship between the contact and elongate pillow forms in the overlying volcanics.

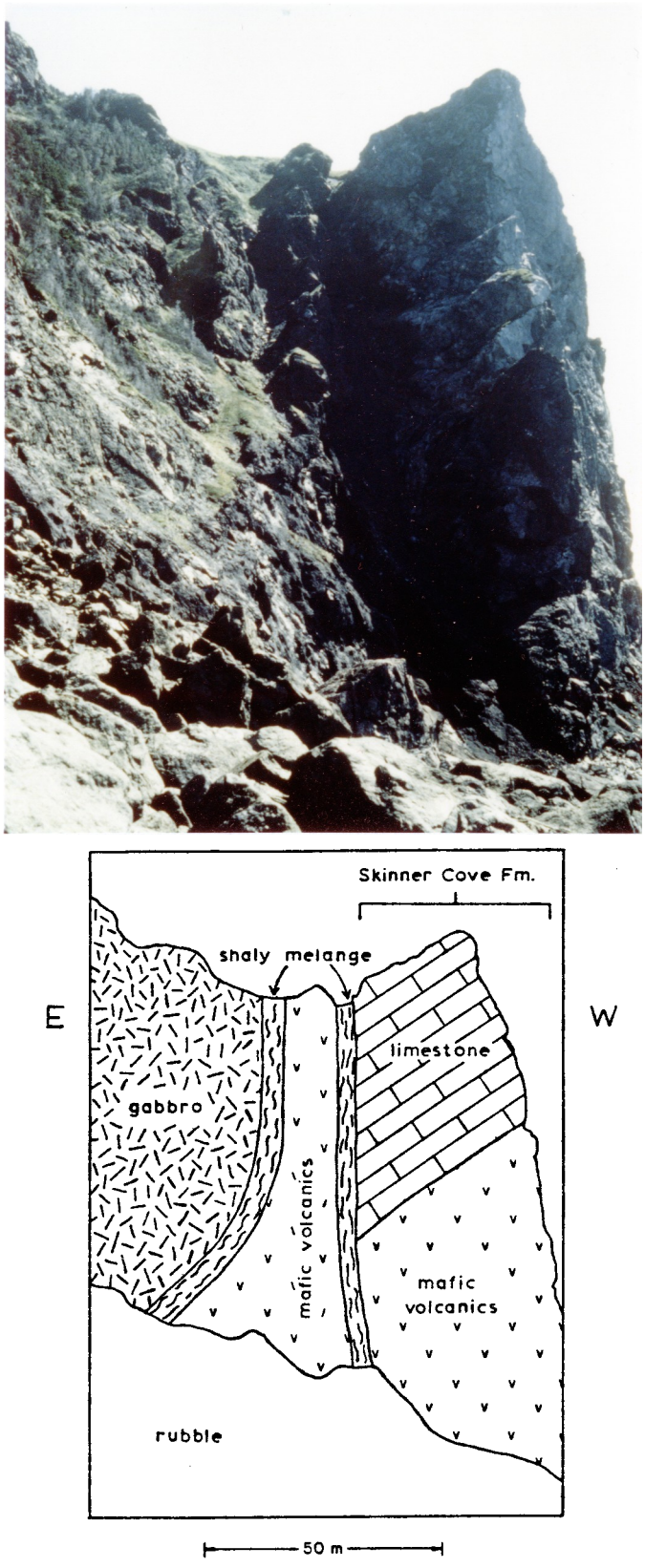

Figure 4.10

Photograph and sketch of the Coastal Complex basal thrust at Chimney Cove Head.

Figure 4.11

Sedimentary melange exposed along the Coastal Complex basal thrust at Chimney Cove. The melange matrix is composed of phacoidally cleaved grey shale, which contains rounded and elongate clasts of pale grey micrite and siltstone. Reddish-brown mafic lava of the Skinner Cove Formation is faulted against the melange near the top of the photo-graph.

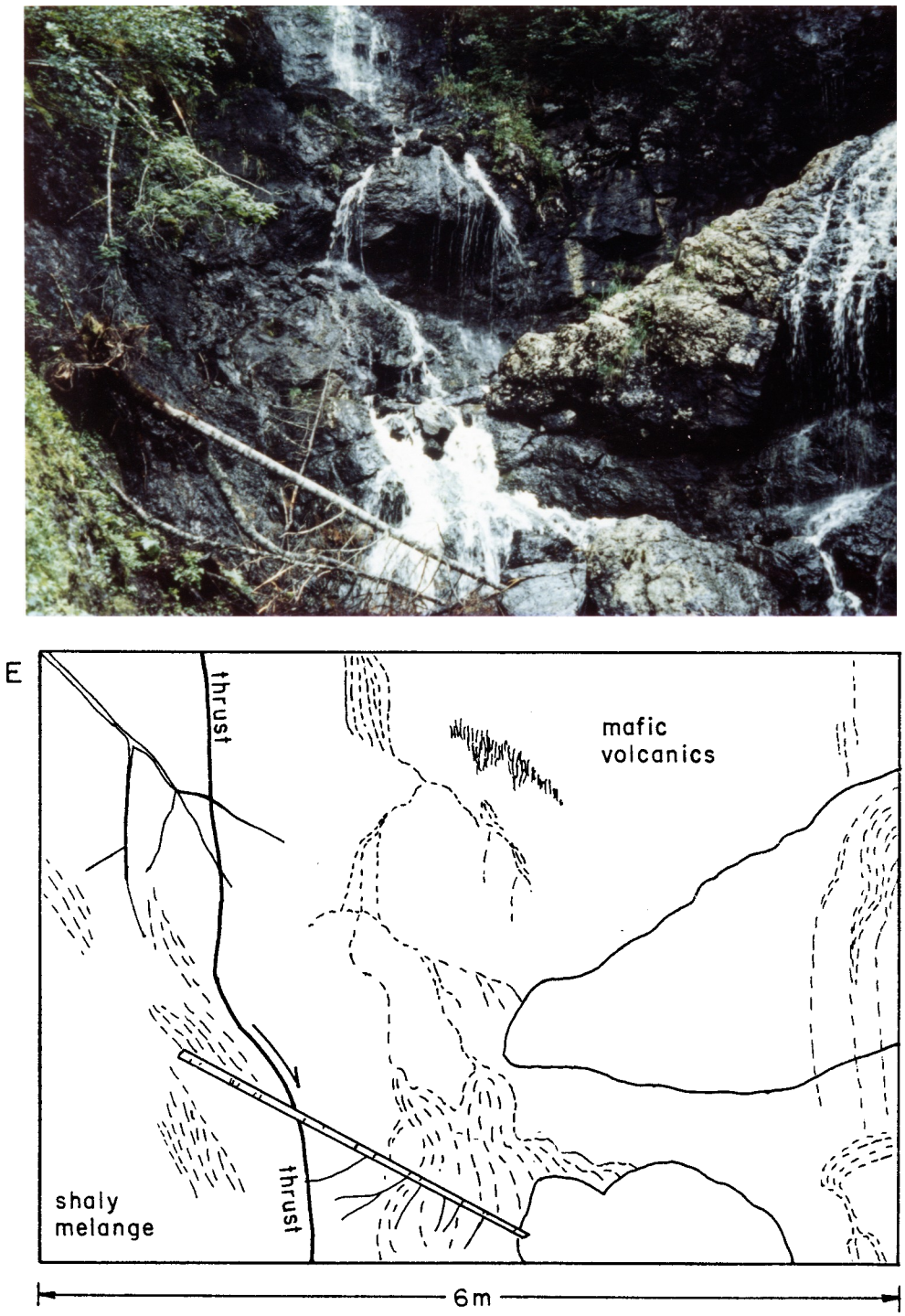

Figure 4.13

Photograph and sketch of the Coastal Complex basal thrust exposure at Alder Bed Brook.

Figure 4.17

View of Devil Head looking westward from the Murray Mountains. Pale grey trondhjemite exposed in the right foreground is separated from reddish-brown felsic volcanic breccia of the Skinner Cove Formation exposed in the background on Devil Head by a small gully that marks the location of the steeply dipping Bottle Cove fault. Another steep fault (the Trumpet Cove fault) separates the trondhjemite from poorly exposed sedimentary melange and volcanics that underlie the low marshy area in the left foreground.

Figure 4.18

View toward the south of the Bottle Cove fault at Parker Beach. Mafic and felsic volcanic rocks of the Skinner Cove Formation comprise Devil Head to the right (west) of the fault, and Coastal Complex trondhjemite forms the cliffs to the left (east). The trondhjemite is separated from sedimentary rocks of the Blow-Me-Down Brook Formation exposed along the shoreline directly below by the Parker Beach fault (buried beneath trondhjemite scree), which is presumed to dip gently into the photograph. The Parker Beach fault appears to be truncated by the subvertical Bottle Cove fault.

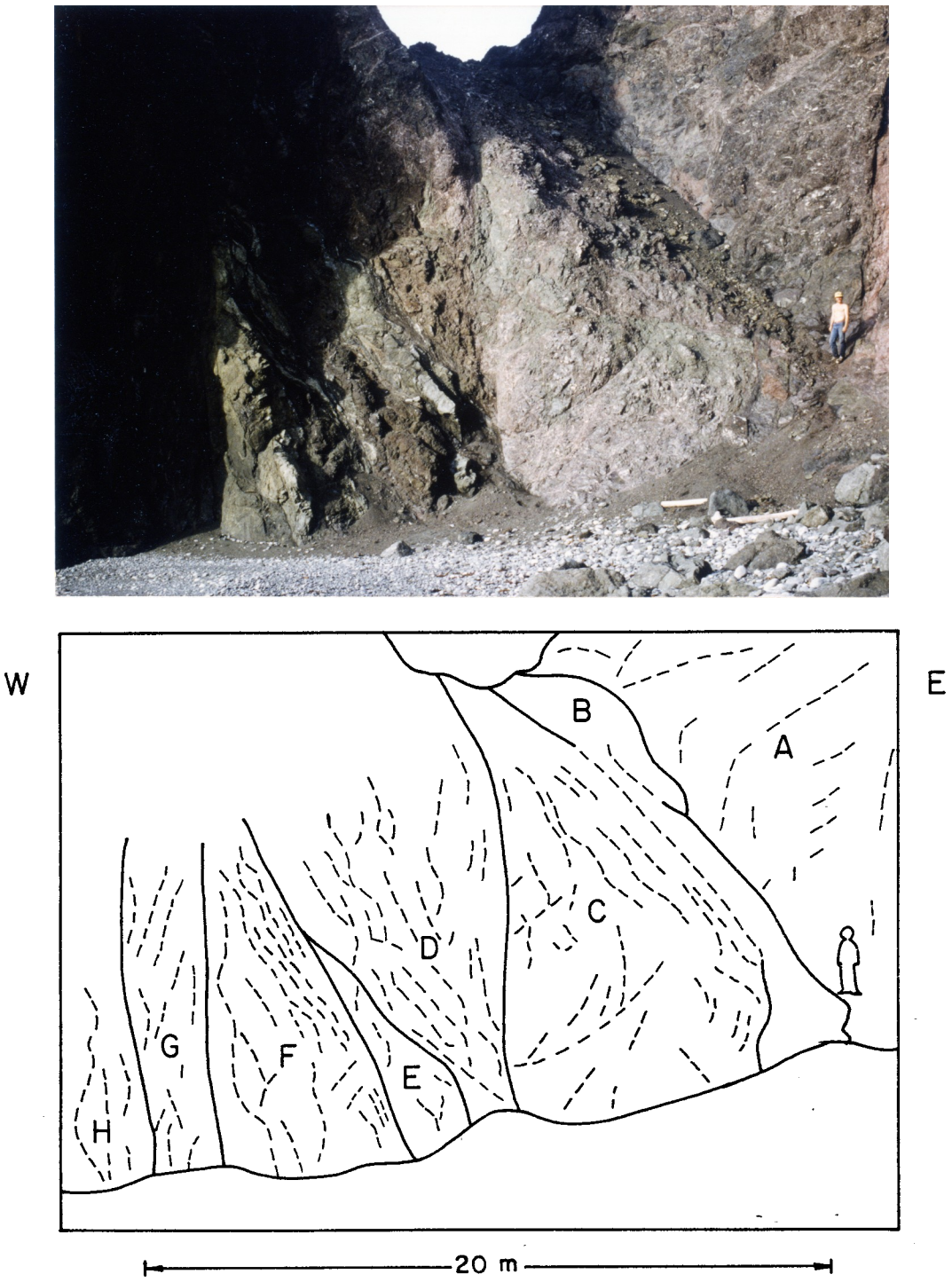

Figure 4.19

Photograph and sketch of the Trumpet Cove fault zone at Trumpet Cove. Legend: (A) red and green weathering, massive and pillowed mafic lavas cut by numerous calcite veins, (B) phacoidally cleaved red mudstone, (C) pale brown weathering, plagioclase-phyric, intermediate to felsic lava with irregular patches of calcite-cemented, sandy to pebbly volcanic breccia and abundant calcite veins, (D) coarse-grained diabase cut by thin dikes of felsic porphyry, (E) reddish-brown weathering, olivine-phyric mafic pillow lava, (F) same as D, (G) phacoidally cleaved melange of fine-grained mafic lava and felsic porphyry, (H) same as D.

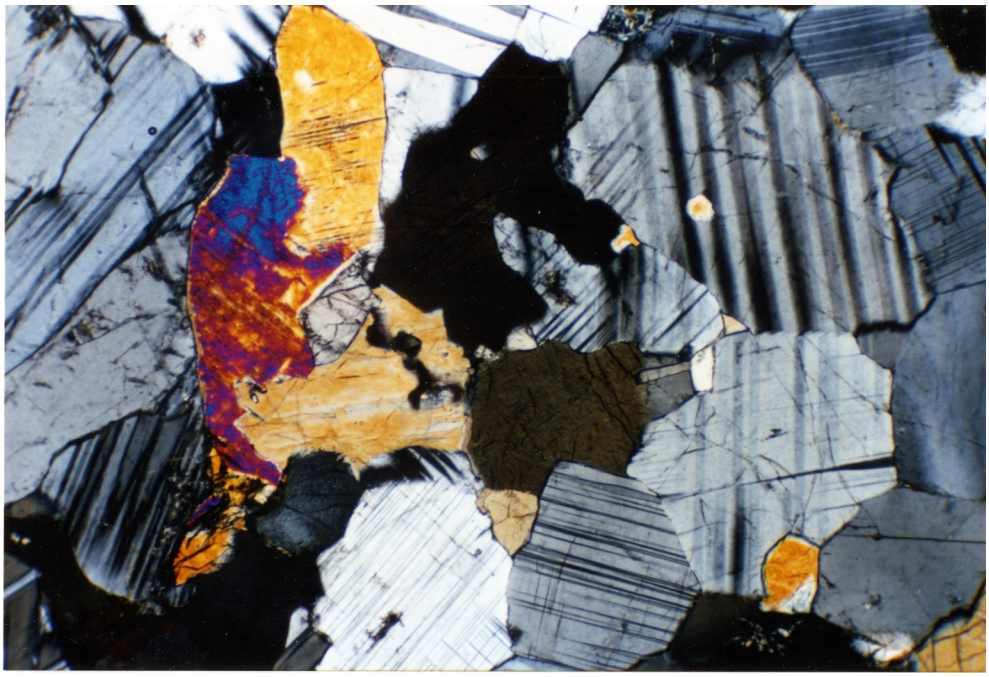

Figure 5.1

Photomicrograph of undeformed clinopyroxene gabbro from Unit 1. Cross-polarized light, long dimension = 2.8 mm.

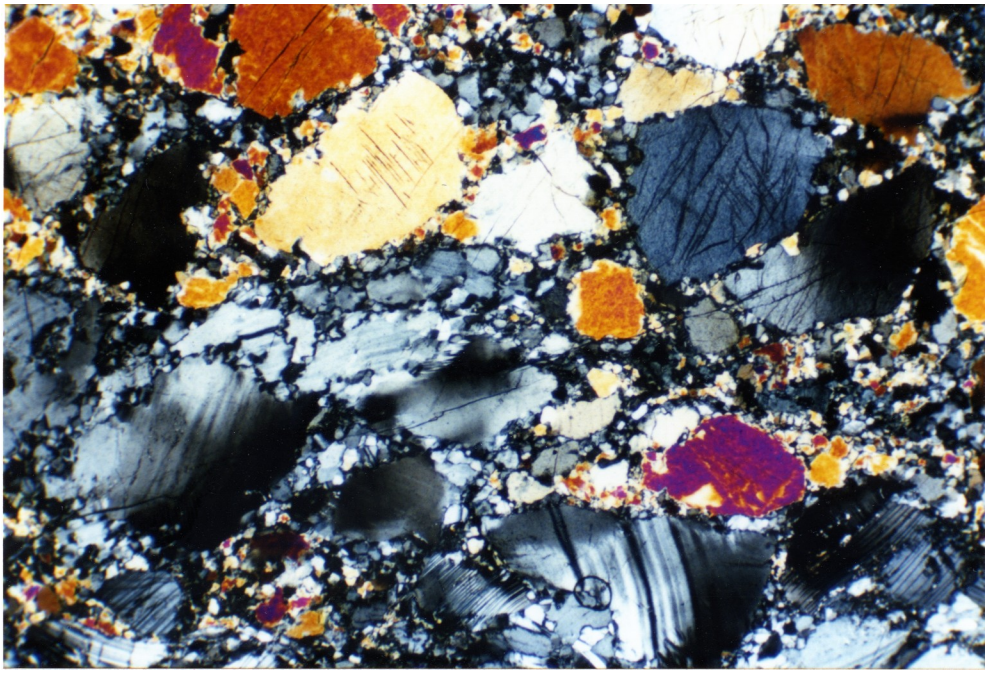

Figure 5.2

Photomicrograph showing partial recrystallization and grain-size reduction in protomylonitic clinopyroxene gabbro from Unit 1. Note bent twins and undulatory extinction in the large relict plagioclase and clinopyroxene grains. Cross-polarized light, long dimension = 2.8 mm.

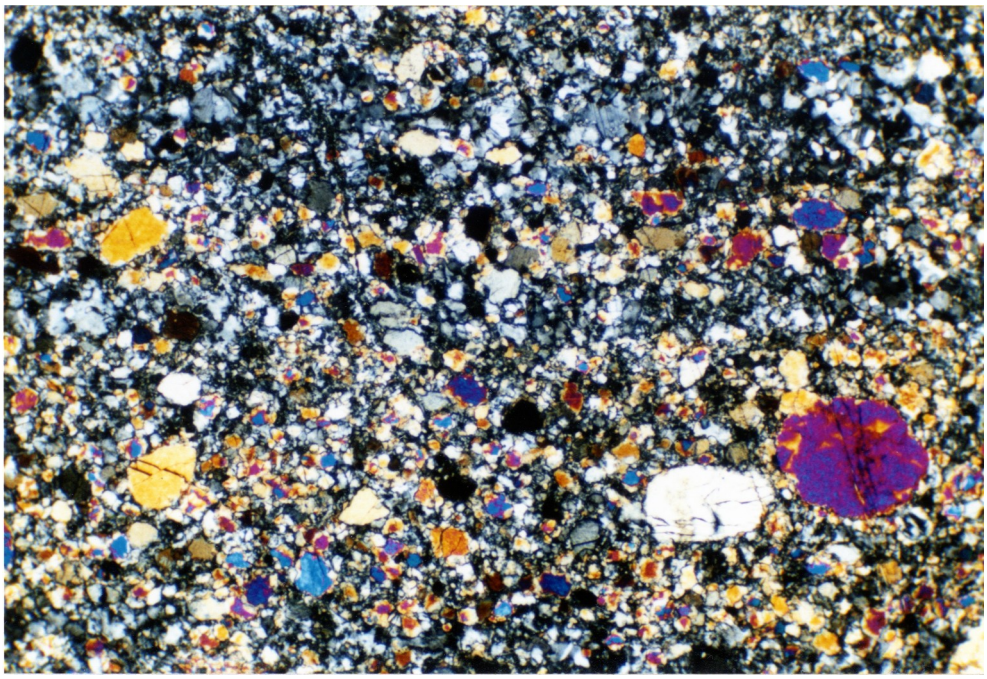

Figure 5.3

Photomicrograph of gabbroic mylonite from Unit 1. Sparse relict clinopyroxene fragments float in a fine-grained matrix of strongly recrystallized plagioclase and clinopyroxene. Cross-polarized light, long dimension = 2.8 mm.

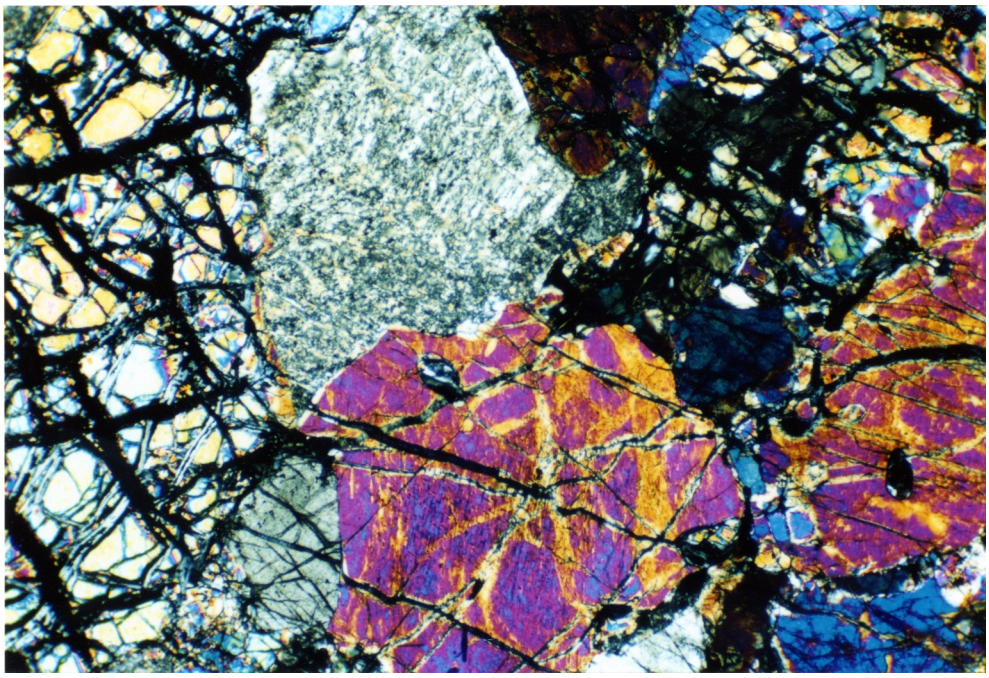

Figure 5.4

Photomicrograph of undeformed plagioclase-bearing wehrlite from Unit 1 containing relatively fresh clinopyroxene, partially serpentinized olivine, and minor sericitized plagioclase (cloudy, turbid grain at top center). Cross-polarized light, long dimension = 2.8 mm.

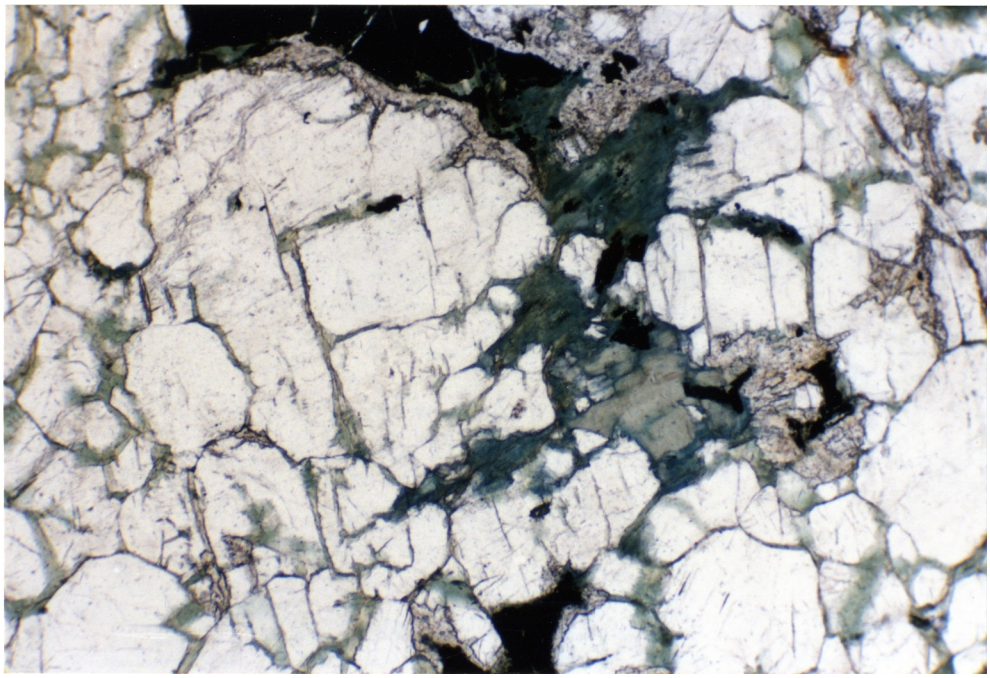

Figure 5.5

Photomicrograph of metagabbro from Unit 1 showing extensive fracturing of plagioclase grains. The fractures are filled with epidote (tan, high relief phase) and blue-green hornblende. Plane-polarized light, long dimension = 2.8 mm.

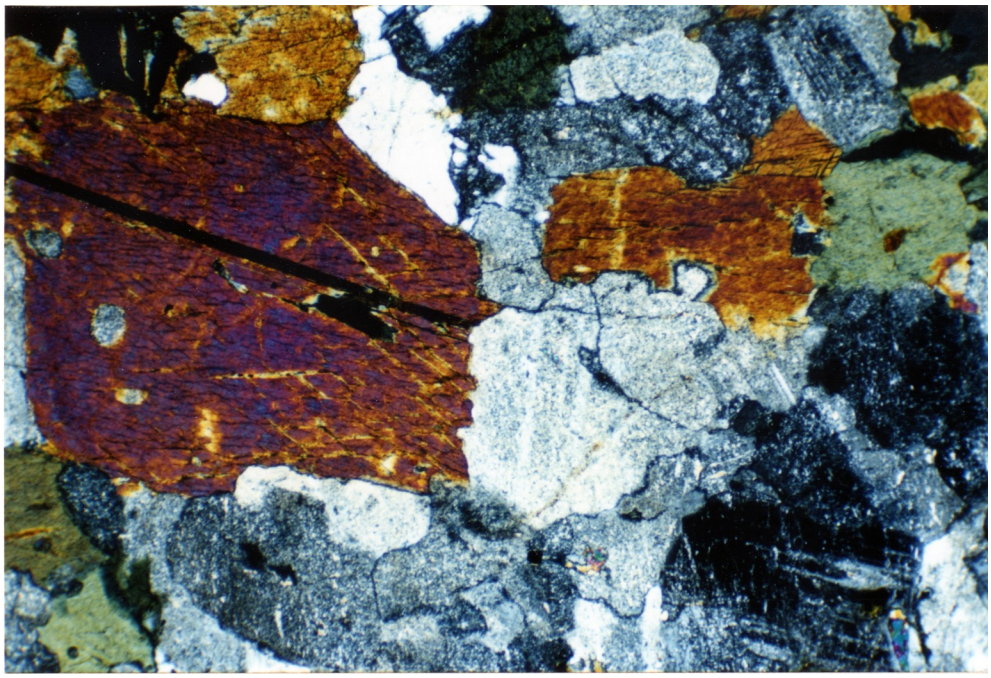

Figure 5.6

Photomicrograph of quartz diorite from Unit 2 containing green hornblende, sericitized plagioclase, and minor quartz (small bright grains at top center). Cross-polarized light, long dimension = 2.8 mm.

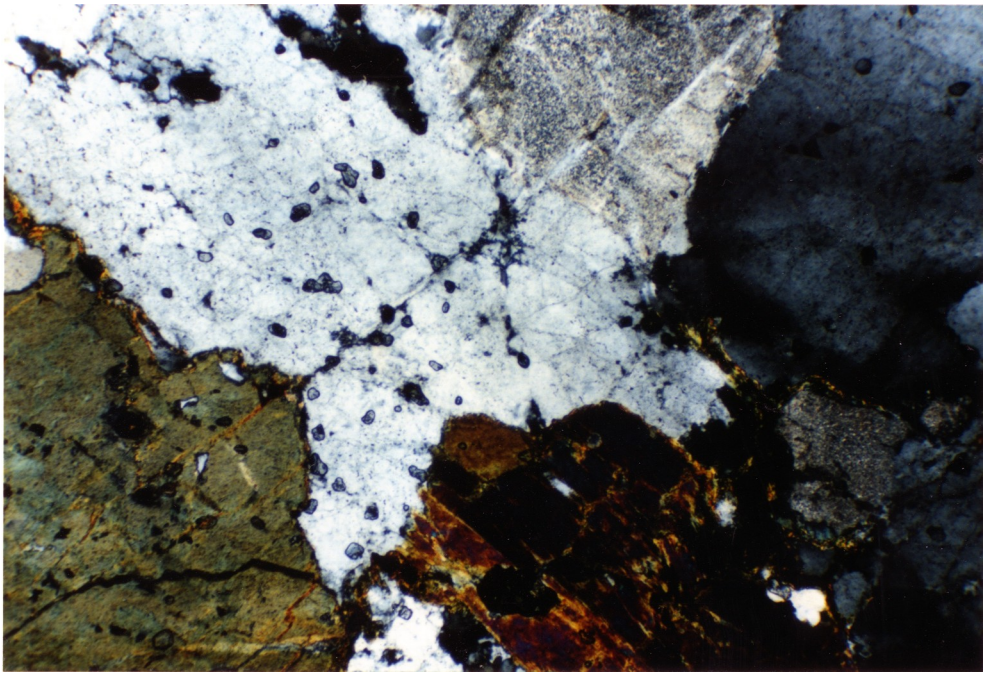

Figure 5.7

Photomicrograph of trondhjemite from Unit 2 containing partially chloritized green hornblende, sericitized plagioclase, and quartz. Note the subgrains and incipient recrystallization in the quartz grains. Cross-polarized light, long dimension = 2.8 mm.

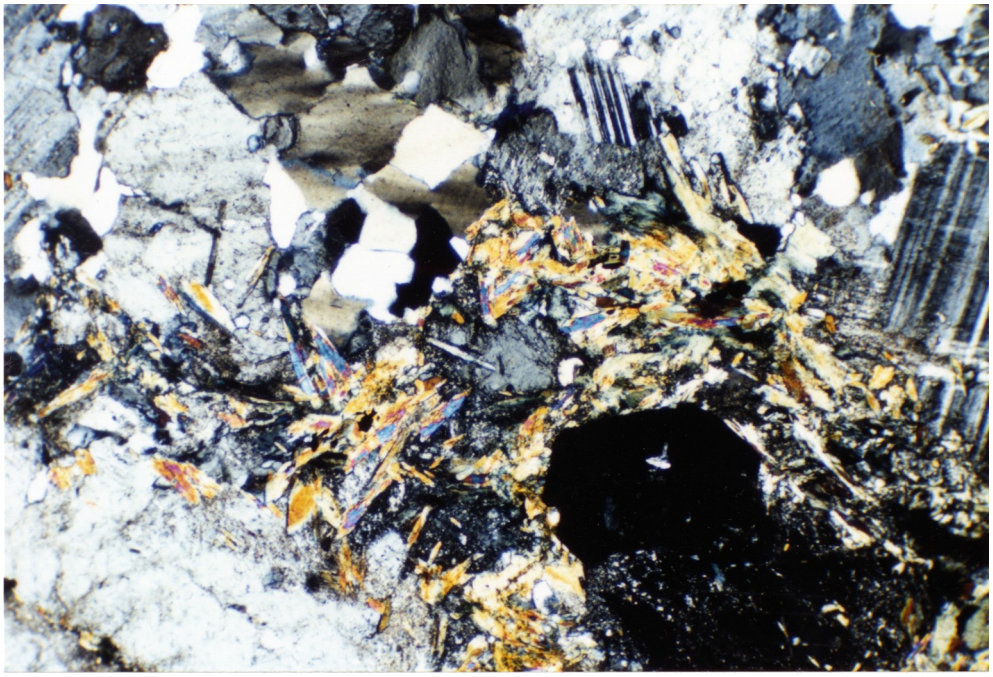

Figure 5.8

Photomicrograph of metatrondhjemite from Unit 2 containing quartz, partially sericitized plagioclase, fibrous green hornblende, and garnet (dark euhedral grain). Cross-polarized light, long dimension = 2.8 mm.

Figure 5.9

Photomicrograph of actinolite schist from Unit 3 showing actinolite-rich and quartz + plagioclase-rich domains. Cross-polarized light, long dimension = 2.8 mm.

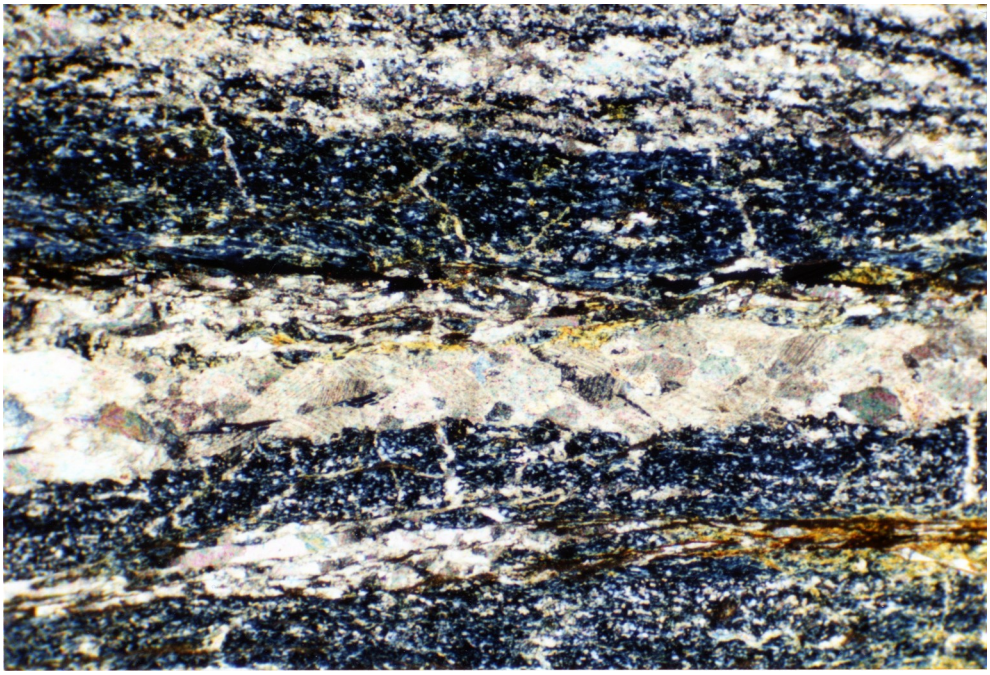

Figure 5.10

Photomicrograph of chlorite schist from Unit 3. This sample contains numerous carbonate-rich bands (tan). The intervening chlorite-rich domains are marked by anomalous dark blue interference colors. Cross-polarized light, long dimension = 2.8 mm.

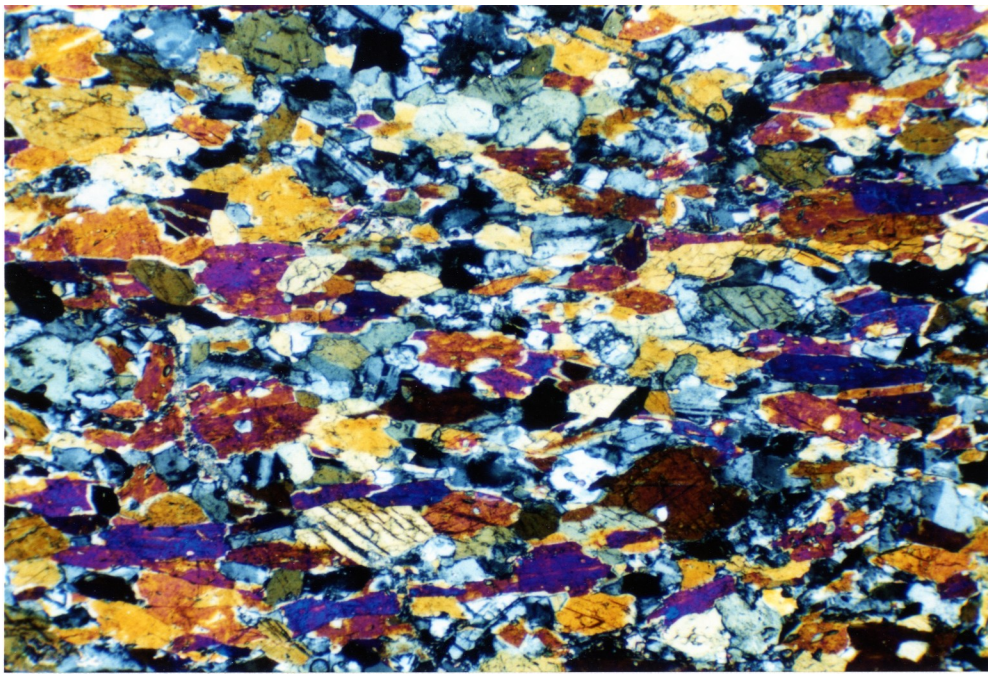

Figure 5.11

Photomicrograph of mylonitic amphibolite from Unit 3 containing blue-green hornblende, plagioclase, minor epidote, quartz, and sphene. Cross-polarized light, long dimension = 2.8 mm.

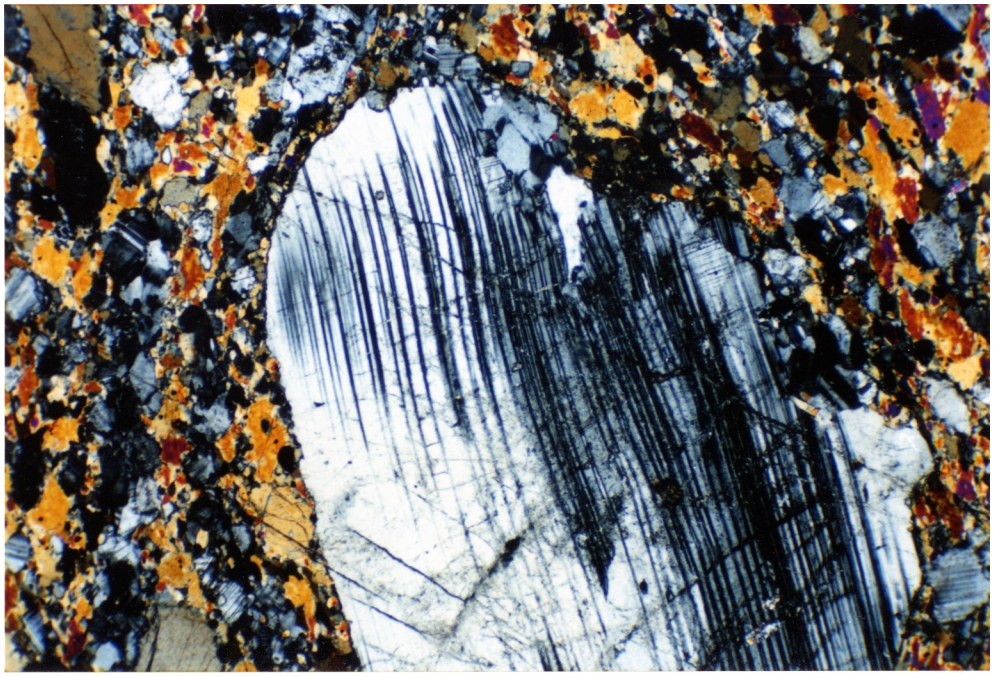

Figure 5.12

Photomicrograph of strained plagioclase porphyroclast in amphibolite from Unit 3. Note the deflection of the foliation around the porphyroclast and the sharp contact between the porphyroclast and matrix. Cross-polarized light, long dimension = 2.8 mm.

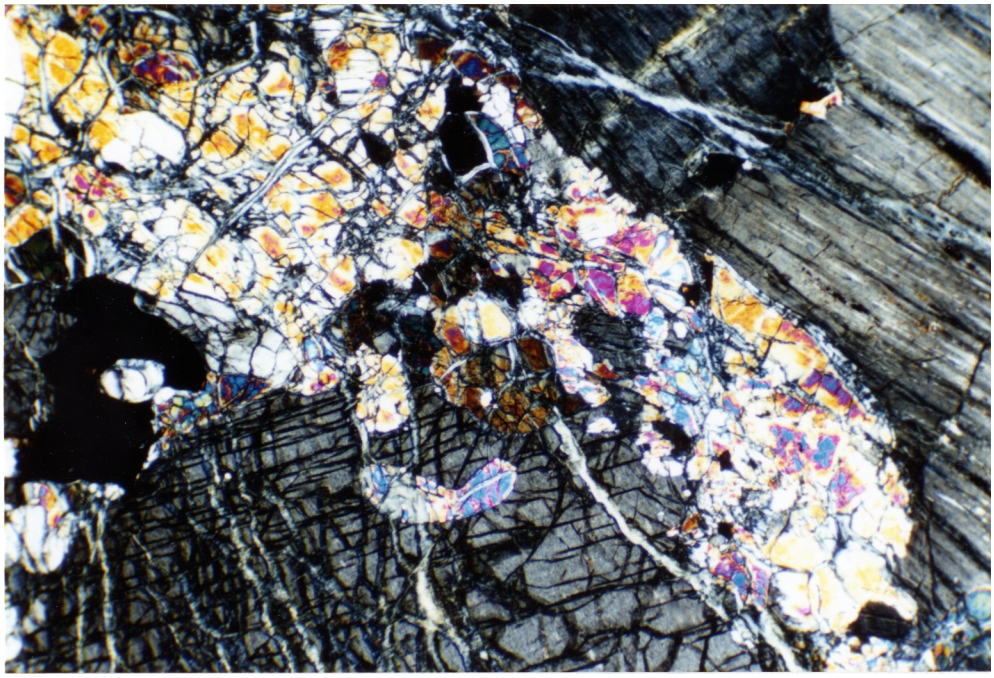

Figure 5.13

Photomicrograph of harzburgite from Unit 4 containing strongly exsolved orthopyroxene, partially serpentinized olivine, and minor chromite (dark). Note the highly embayed grain shapes (particularly noticable in chromite) and the blebs of olivine in orthopyroxene. Cross-polarized light, long dimension = 2.8 mm.

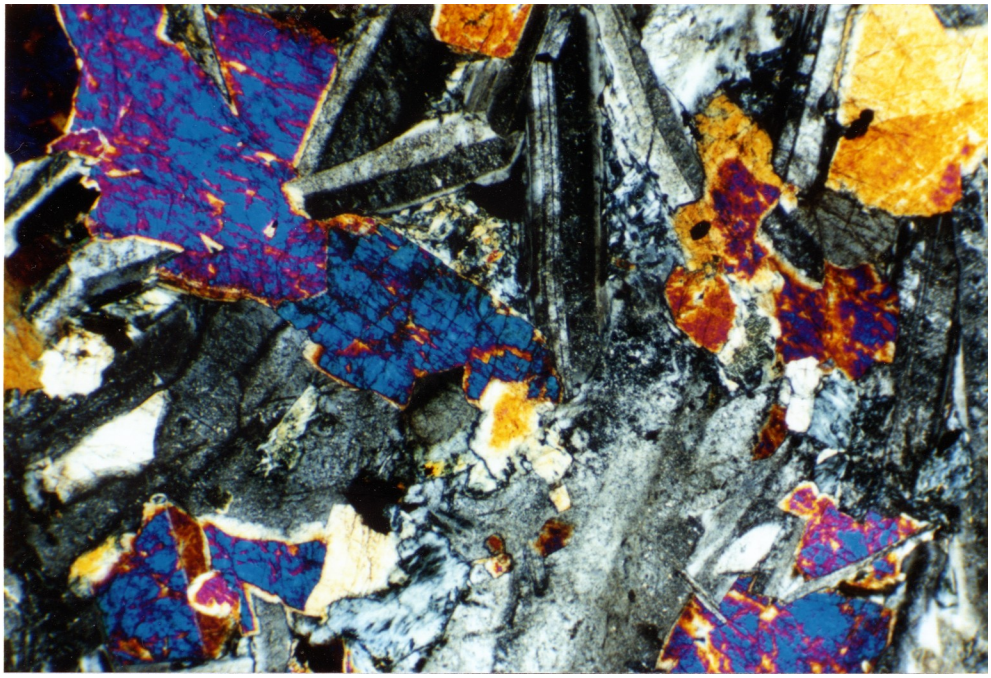

Figure 5.14

Photomicrograph of coarse-grained diabase dike associated with Unit 5. Anhedral to subhedral clinopyroxene grains (some rimmed by brown hornblende) occupy the interstices between dusty, sericitized plagioclase laths. Note the small chlorite patches (grey-blue) near center and bottom center. Cross-polarized light, long dimension = 2.8 mm.

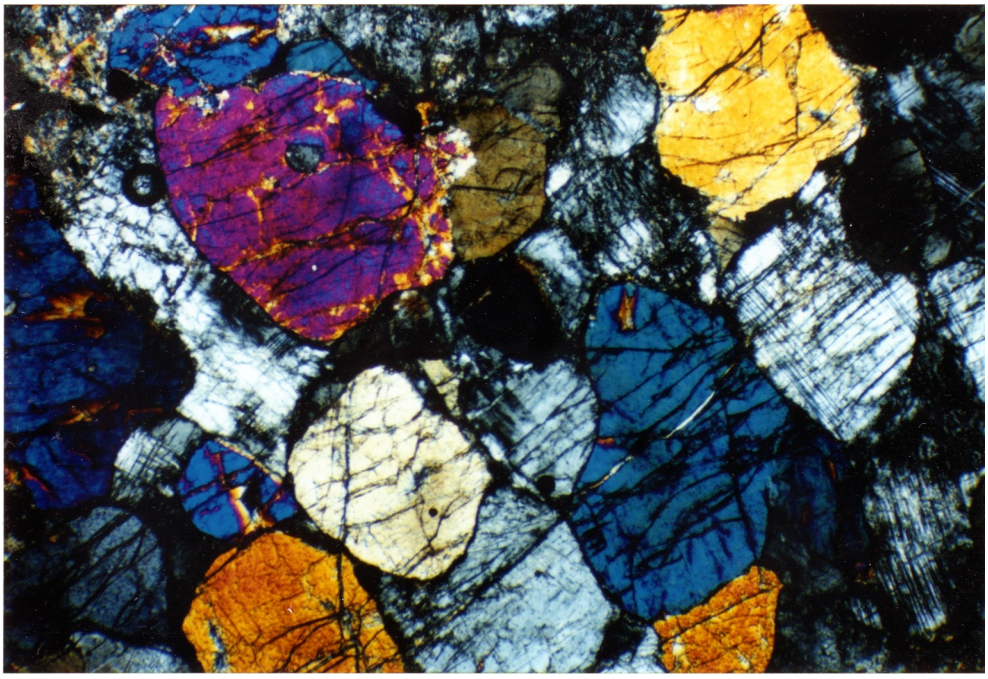

Figure 5.15

Photomicrograph of undeformed clinopyroxene gabbro from Unit 5. Cross-polarized light, long dimension = 2.8 mm.

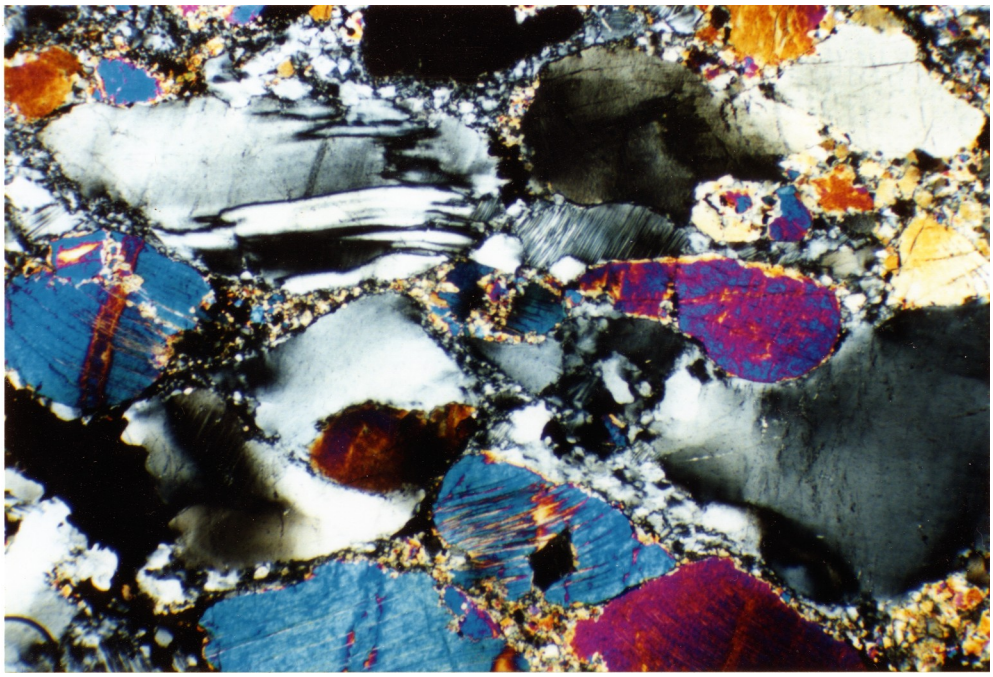

Figure 5.16

Photomicrograph of protomylonitic gabbro from Unit 5. Highly strained relict grains of plagioclase, clinopyroxene, and minor brown hornblende are surrounded by thin mantles of fine recrystallized grains. Cross-polarized light, long dimension = 2.8 mm.

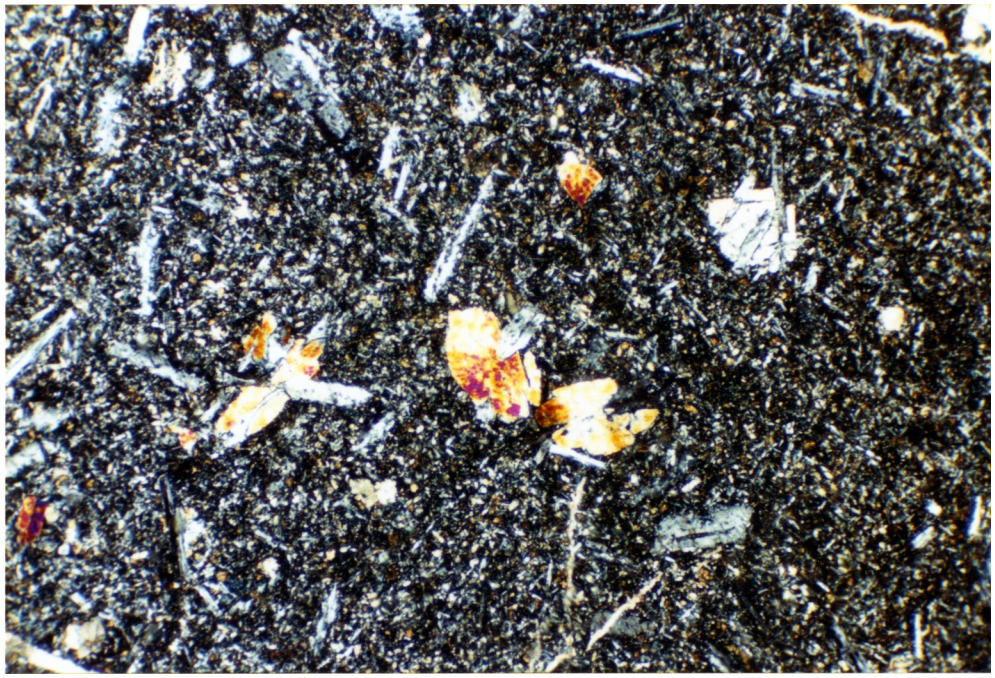

Figure 5.17

Photomicrograph of little-altered mafic volcanic rock from Unit 6 containing microphenocrysts of plagioclase and clinopyroxene. The matrix is also composed primarily of plagioclase and clinopyroxene, along with minor amounts of chlorite, calcite, and an Fe-Ti oxide phase. Cross-polarized light, long dimension = 2.8 mm.

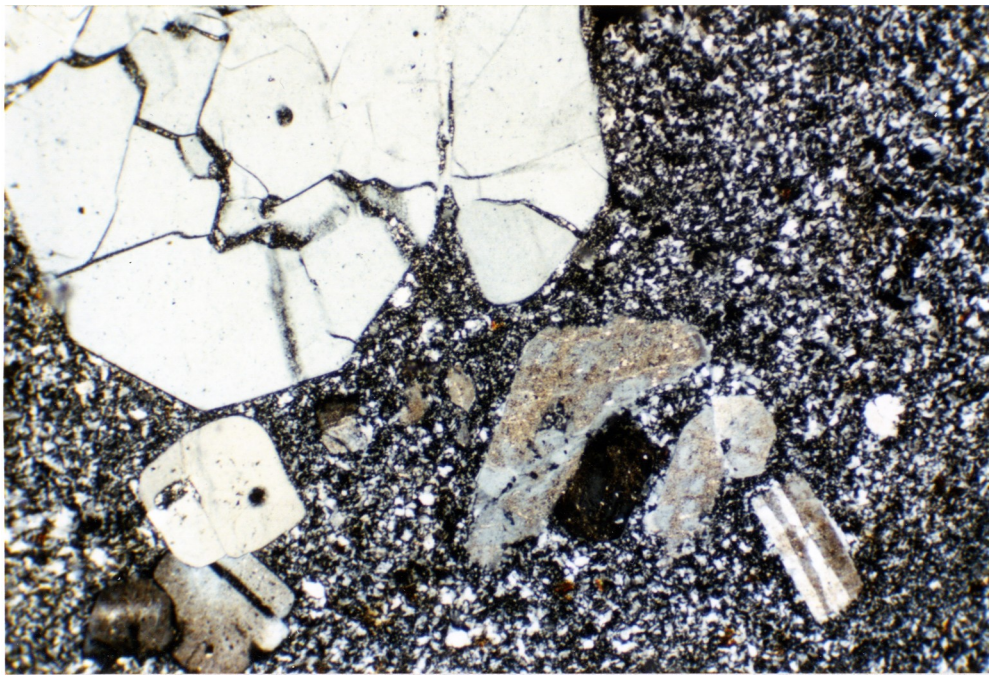

Figure 5.18

Photomicrograph of felsic volcanic rock from Unit 6 containing euhedral phenocrysts of quartz (bright fractured grains) and sericitized plagioclase (dusty). Cross-polarized light, long dimension = 2.8 mm.

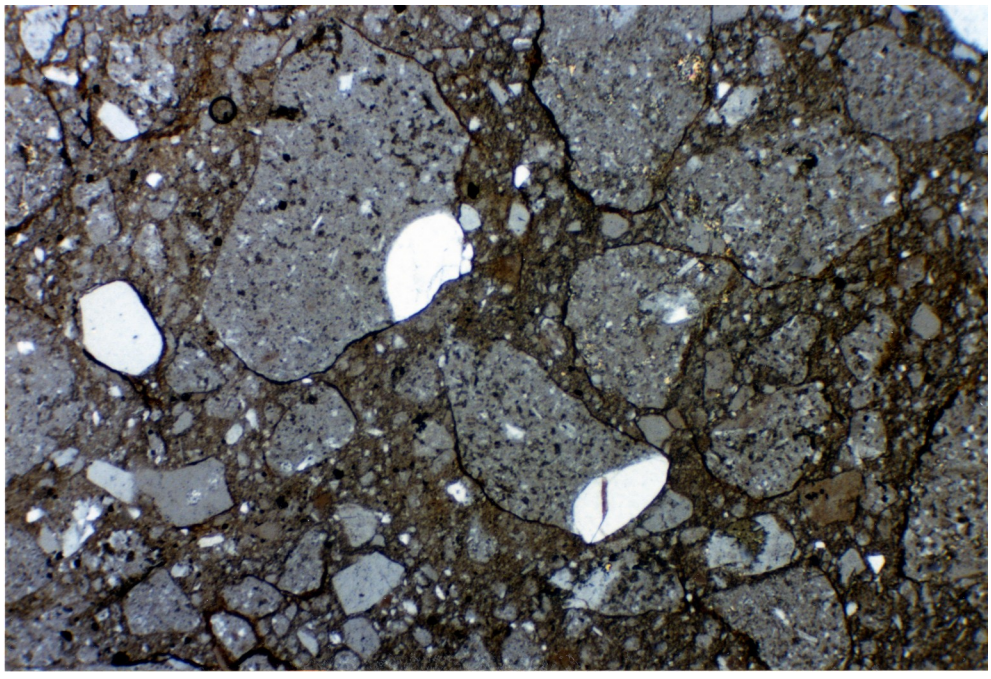

Figure 5.19

Photomicrograph of felsic microbreccia from Unit 6. The large bright grains in the clasts and matrix are quartz phenocrysts. Polars crossed 20°, long dimension = 2.8 mm.

Figure 6.1

Compositional layering in olivine gabbro (brown) and anorthositic gabbro (pale grey) of Unit 1. The diameter of the lens cap in this and subsequent photographs equals 6 cm.

Figure 6.2

Compositional layering in feldspathic wehrlite (brown) and anorthosite (pale grey) of Unit 1. This outcrop contains a well-developed layer-parallel S_{1a} foliation.

Figure 6.3

Undeformed, plagioclase-phyric diabase dike (reddish brown) cutting S_{1a} foliation in gabbro (grey) of Unit 1.

Figure 6.4

Small S_{1b} ductile shear zone (strongly foliated band in center of photograph) in melagabbro of Unit 1. The apparent clockwise deflection of the foliation toward the shear zone suggests that movement along the zone was dextral in this view.

Figure 6.5

Open, cylindrical F_3 fold in lineated gabbro of Unit 1.

Figure 6.6

Small diabase dike cutting undeformed gabbro of Unit 1.

Figure 6.7

Irregular, undeformed trondhjemite dike cutting weakly foliated gabbro of Unit 1.

Figure 6.8

Pink aplite vein in Unit 2 trondhjemite at Parker Beach.

Figure 6.9

Irregular diabase dikes cutting trondhjemite at South Head. The dikes feed overlying massive and brecciated mafic lavas of Unit 6 in the upper portion of the photograph.

Figure 6.10

Chilled margins on diabase dike cutting trondhjemite of Unit 2 at South Head.

Figure 6.11

Irregular patches of diabase in trondhjemite at South Head.

Figure 6.12

Screen of coarse-grained trondhjemite bounded by strongly chilled diabase dikes at White Point.

Figure 6.13

L_{2a} lineation in an outcrop of strongly deformed metatrondhjemite near Trout River.

Figure 6.14

Strong S_{2a} foliation (parallel with notebook) and L_{2a} mineral elongation lineation (trends NE-SW in plane of foliation) in amphibolite of Unit 3.

Figure 6.15

Plagioclase porphyroclast-rich layer in foliated (S_{2a}) amphibolite of Unit 3. Several of the large porphyroclasts above and to the left of the lens cap are noticeably asymmetric.

Figure 6.16

Well-developed structural/metamorphic layering in greenschist-facies metabasites of Unit 3 at Pigeon Cove. The pale layers are composed of weakly foliated metagabbro. The darker layers of mylonitic actinolite schist represent planar S_{2b} shear zones. Note the large F_2 intrafolial fold approximately 2 meters above K. Idleman.

Figure 6.17

Curviplanar S_{2b} shear zone developed in coarse-grained metagabbro on Pigeon Island. The fold-like structures in the shear zone are strongly disharmonic and do not significantly affect the weak S_{1a} foliation and cm-scale S_0 compositional layering seen in the metagabbros beneath the lens cap.

Figure 6.18

Asymmetric phacoids of coarse-grained metagabbro in a S_{2b} shear zone on Pigeon Island.

Figure 6.19

F_2 intrafolial folds of fine-grained trondhjemite lenses in Unit 3 amphibolite.

Figure 6.20

Tight F_2 folds of S_{2a} schistosity and fine-grained carbonate ("marble") bands in chlorite schist.

Figure 6.21

Relationship between F_2 and F_3 folds on Pigeon Island. An intrafolial F_2 fold developed in the S_{2b} shear zone beneath the lens cap has been folded about an open F_3 fold with a steeply dipping axial plane. The surface of this outcrop is approximately perpendicular to both the F_3 fold axes and the L_{2a} mineral elongation lineation developed in the shear zone, which plunge moderately toward the southeast. The F_2 fold appears to have a double closure in this view, suggesting that it may be a sheath fold elongated in the direction of the lineation.

Figure 6.22

F_3 folds in actinolite schist on Pigeon Island. Note the difference in style between the large cylindrical fold in the center of the photograph and smaller, more angular parallel folds to the right. The length of the hammer handle is about 35 cm.

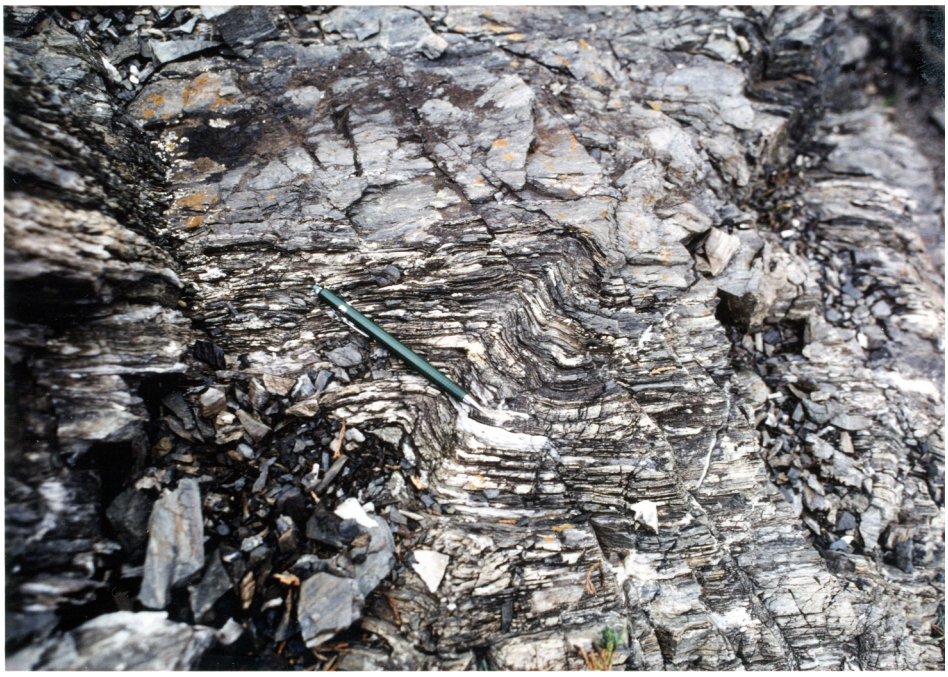

Figure 6.23

F_4 kink band in chlorite schist of Unit 3.

Figure 6.24

Fine-grained, undeformed felsite dike cutting S_{2a} foliation in amphibolite of Unit 3.

Figure 6.25

Undeformed, 2 meter thick diabase dike cutting actinolite schist and metagabbro of Unit 3 on Pigeon Island. The small jog in the dike seen near the center of the photograph may be related to F_3 folding, since F_3 folds are well developed in the metabasites immediately above this portion of the dike.

Figure 6.26

Partially deformed metadiabase dike on Pigeon Island. The dike exhibits an irregular chilled margin against weakly foliated metagabbro near the bottom the photograph. Its upper margin is marked by a narrow S_{2b} shear zone.

Figure 6.27

Irregular contact between a moderately foliated metadiabase dike (dark maroon-grey) and strongly foliated actinolite schist (pale grey) on Pigeon Island.

Figure 6.28

View toward the southeast over the Trumpet Cove melange zone from the Murray Mountains. Most of the exposures along the floor of the valley are composed of grey-weathering diabase and microgabbro, which occur as dikes and fault-bounded slivers in the melange. Several small outcrops of pale orange weathering harzburgite are also visible. Gabbro and trondhjemite of the Monkeylands massif are exposed on the opposite side of the valley. In the distance, the Blow-Me-Down Mountain massif of the Bay of Islands complex is visible along the skyline beyond York Harbour and Governours Island.

Figure 6.29

Large block of orange-weathering harzburgite in phacoidally cleaved grey-green serpentinite at Trumpet Cove.

Figure 6.30

Isoclinal folds of orthopyroxenite layers in harzburgite from a block in the Trumpet Cove melange.

Figure 6.31

Partially dismembered diabase dike in sheared serpentinite at Trumpet Cove. The dike exhibits well-developed chilled margins in the left half of the photograph but is sharply faulted against serpentinite to the right.

Figure 6.32

Small, steeply dipping megadike of reddish brown microgabbro near Pissing Mare Cove. The megadike is about 5 meters high and cuts layered grey gabbro and anorthosite of Unit 1, which are exposed along its base. A much larger megadike is exposed at the top of precipitous cliffs above the scree slope in the background.

Figure 6.33

Regionally extensive megadike of Unit 5 gabbro exposed in coastal cliffs above Rencontre Cove. Layered gabbroic rocks of Unit 1 are exposed along the shoreline in the foreground.

Figure 6.34

Xenolith of coarse-grained, foliated gabbro (grey), possibly derived from Unit 1, in undeformed microgabbro (reddish-brown) of Unit 5.

Figure 6.35

Compositional layering in coarse-grained gabbro of Unit 5.

Figure 6.36

Irregular contact between a regionally extensive microgabbro megadike (brown) and coarse-grained gabbro of Unit 1 (grey) exposed along the coastline northeast of Rencontre Cove. The microgabbro grades into a zone of flinty, chilled diabase about 50 cm thick along the margin of the megadike. The length of the hammer handle is about 35 cm.

Figure 6.37

Exposure of mafic pillow lava in Unit 6.

Figure 6.38

Mafic pillow breccia in Unit 6. The matrix of the breccia is composed of sandy, calcite-cemented volcaniclastic material.

Figure 6.39

Strongly altered and veined gabbro of Unit 1 exposed along the west side of Lark Harbour. This locality lies several meters below the basal contact of Unit 6.

Figure 6.40

Gabbro breccia developed directly beneath the basal contact of Unit 6.

Figure 6.41

Contact between pebbly mafic volcanic breccia (above) and gabbro breccia (below hammer head) exposed along the west side of Lark Harbour. The contact is intruded by a diabase sill at the level of the hammer handle.

Figure 8.3

Undeformed postkinematic diabase dike (subvertical pale orange band to the right of the lens cap) cutting fine-grained, strongly foliated amphibolite (grey) of the metamorphic aureole northeast of Table Mountain (locality A, Figure 8.2).

Figure 8.4

Strongly foliated pre- to synkinematic diabase dike (orange band below lens cap) cutting fine-grained, foliated amphibolite (grey-brown) of the metamorphic aureole northeast of Table Mountain (locality A, Figure 8.2). The dike is subparallel with the foliation in the amphibolite and is offset by about 10 cm along a subvertical fracture to the left of the lens cap.